

## Holographic three-dimensional polymeric photonic crystals operating in the 1550 nm window

Jiaqi Chen, Wei Jiang,<sup>a)</sup> Xiaonan Chen, Li Wang, Sasa Zhang, and Ray T. Chen<sup>b)</sup>  
 Microelectronics Research Center, Department of Electrical and Computer Engineering,  
 The University of Texas at Austin, Austin, Texas 78758

(Received 12 December 2006; accepted 23 January 2007; published online 26 February 2007)

A polygonal prism based holographic fabrication method has been demonstrated for a three-dimensional face-centered-cubic-type submicron polymer photonic crystal using both positive and negative photoresists. Special fabrication treatments have been introduced to ensure the survivability of the fabricated large area ( $\sim 1 \text{ cm}^2$ ) nanostructures. Scanning electron microscopy and diffraction results proved the good uniformity of the fabricated structures. With the proper design of the refraction prism the authors have achieved the required band gap for  $S+C$  bands (1460–1565 nm) in the [111] direction. The transmission and reflection spectra obtained by Fourier transform infrared spectroscopy are in good agreement with simulated band structure. © 2007 American Institute of Physics. [DOI: 10.1063/1.2709641]

The prediction and the confirmation that periodic dielectric structures can be used to manipulate electromagnetic wave propagation affect significantly the development of the micro- and nano-optoelectronics.<sup>1–5</sup> There is a great diversity in the fabrication approaches for making two-dimensional and three-dimensional photonic crystals. Despite the remarkable progress in the fabrication of two-dimensional photonic crystals,<sup>6</sup> there remain significant challenges for the fabrication of three-dimensional (3D) photonic crystals. Many fabrication approaches have been studied. Among them, layer-by-layer stacking using nanoimprint,<sup>7</sup> microassembly of planar semiconductor layers<sup>8</sup> and multiphoton absorption<sup>9</sup> have been investigated to create certain microstructures. However, for the aforementioned approaches multiple processing steps are generally required and they are not suitable for larger scale ( $\text{cm}^2$  size) fabrication.

Recently, after Campbell *et al.*<sup>10</sup> demonstrated the holographic fabrication of 3D photonic crystal, holographic lithography has gained more attention in the fabrication of 3D polymer photonic crystals. By controlling the multiple laser beams one can generate a desired 3D interference pattern to expose the photoresist and render the exposed area soluble or insoluble depending on the material type in use. And it has been proven theoretically that all 14 Bravais lattices can be constructed using such a method.<sup>11</sup> In the early days of this approach multiple beams were formed by independent optical components. Such setups were complicated and required careful alignment. Recently, Divliansky *et al.*<sup>12</sup> introduced a diffraction mask to create the four desired beams and Wu *et al.*<sup>13</sup> demonstrated another idea using a single refracting prism to split and combine the desired beams. With the use of a single optical element, sophisticated antivibration system and alignment are avoided. However, the photonic band gap effect of most of these devices created by a single optical element did not fall in the optical communication windows due to the relatively large period. Here based on the diffraction prism approach we used a He–Cd dual wavelength laser to fabricate submicron 3D photonic crystal structure using

the negative  $i$ -line resist SU8 with a 325 nm wavelength and the positive  $g$ -line resist AZ4620 with a 442 nm wavelength.

The optical setup for the fabrication using SU8 is illustrated in Fig. 1(a). The ultraviolet (UV) laser beam coming from the He–Cd laser was expanded using on UV objective lens. The spatial filter afterward cleaned up the unwanted scattering in the optical path to ensure a good beam quality. After the laser beam was collimated it hit normally on the specially designed top-cut prism. The three sidewalls of the prism created three side beams by beam refraction. The center beam of this umbrella interference configuration was formed from the central part of the collimated laser beam going through the top and bottom surfaces of the prism. The four beams overlapped at the bottom of the prism. In our design shown in Fig. 1(b),  $L_1=1 \text{ cm}$ ,  $L_2=4 \text{ cm}$ , and  $H=1.5 \text{ cm}$ . The resulting wave vectors were  $G_0=2\pi/\lambda(0,0,-1)$ ,  $G_1=2\pi/\lambda(-0.331,-0.191,-0.9234)$ ,  $G_2=2\pi/\lambda(0.331,-0.191,-0.924)$ , and  $G_3=2\pi/\lambda(0,0.383,-0.924)$ , where  $\lambda=325 \text{ nm}$  for the use of SU8 and 442 nm for the use of AZ4620. The interference pattern can be calculated by

$$I(\mathbf{r}) = \sum_{i=0}^{N-1} E_i^2 + 2 \sum_{i=1}^{N-1} E_0 \times E_i \times \mathbf{e}_0 \cdot \mathbf{e}_i \times \cos(\mathbf{K}_i \cdot \mathbf{r} + \theta_i) \\ + 2 \sum_{i>j=1}^{N-1} E_i \times E_j \times \mathbf{e}_i \cdot \mathbf{e}_j \times \cos(\mathbf{K}_{ij} \cdot \mathbf{r} + \theta_{ij}),$$

where  $K_i=G_i-G_0$ ,  $K_{ij}=K_i-K_j$ ,  $\theta_{ij}=\theta_i-\theta_j$ ,  $N=4$ , and  $\theta_i$ , is

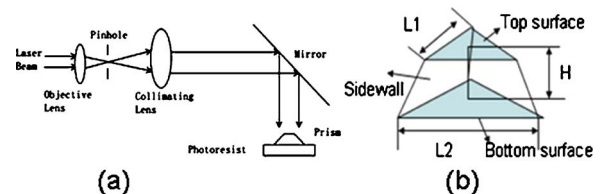


FIG. 1. (Color online) (a) Schematic of the holographic lithography setup. The collimated laser beam is reflected by a mirror towards the prism and the glass substrate. (b) Coupling prism has a symmetric structure. The top and bottom surfaces are equilateral triangles with edges of  $L_1$  and  $L_2$ , respectively.

<sup>a)</sup>Present address: Omega Optics, Inc., Austin, TX 78758.

<sup>b)</sup>Electronic mail: raychen@uts.cc.utexas.edu

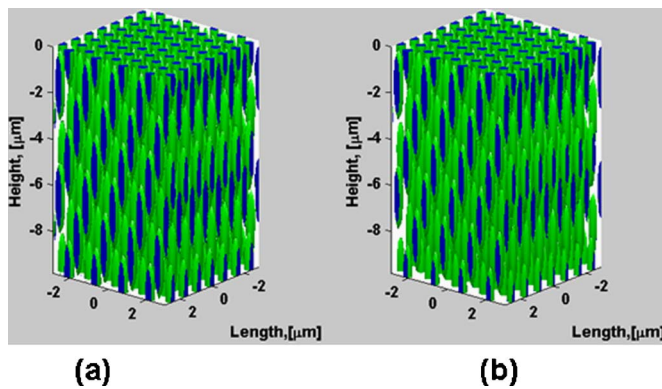


FIG. 2. (Color online) (a) Simulation of intensity distribution in the photoresist without considering the absorption. (b) Simulation of intensity distribution in the photoresist considering the absorption.

the phase difference of the beam relative to the center beam. With the polarization of the incident laser beam aligned with the  $x$  axis in the system, the resulting polarizations for the four beams are  $\mathbf{e}_0=(1,0,0)$ ,  $\mathbf{e}_1=(0.941,0.06,-0.339)$ ,  $\mathbf{e}_2=(0.941,-0.06,0.339)$ , and  $\mathbf{e}_3=(1,0,0)$ .

In the fabrication a bottom black glass plate was used to reduce the back reflection and all the interfaces used index matching liquid to avoid the unwanted reflections at the glass/air and polymer/air interfaces.

To model the 3D holographic lithography process more accurately we need to consider the absorption inside the photoresist.<sup>14</sup> With reduced size, the reliability of the fabricated structures would be more influenced by such absorption. Figures 2(a) and 2(b) show the computer simulations of a fcc (face-centered-cubic)-type photonic crystal structure with and without absorption using the  $K$  vectors obtained before and an SU8 absorption of  $0.1/\mu\text{m}$  at 330 nm. The blue volume enclosed by the green surface has an exposure dosage above the polymerization threshold and would be insoluble after development for a negative resist. Particularly, it is critical to ensure good substrate adhesion and avoid the structural damage originating from the capillary drainage of the rinsing liquid during the drying process for a small feature size structure.<sup>15</sup> From the simulation results with the absorption, it is obvious that the bottom part of the resist receives less dosage. Therefore less resist would remain at the bottom part after development, and it is highly susceptible to damage. The standard SU8 rinsing liquid is isopropanol with a surface tension  $\gamma$  of 23 mN/m and a contact angle  $\theta=20^\circ$ . On the contrary, when considering the wetting characteristic, although de-ionized (DI) water has a higher surface tension of 73 mN/m, it has a contact angle of  $81^\circ$ . As the capillary force is proportional to  $\gamma\cos(\theta)$ , the capillary force exerted by water is about twice smaller than that by isopropanol. Then we switched to DI water as the rinse liquid for all the samples, and no peel off was observed.

For a positive resist, the exposed volume will be removed during development. With the absorption there is a decrease of dissolution volume with the increased depth of photoresist. Moreover, the effective development time for the upper resist is longer than that for the lower part. Combining these two effects, we would have overdeveloped and damaged the top structures before the desired 3D structure is formed at the lower part of the resist. So we have flipped the recording glass plate and let the laser beams incident on the glass substrate at first then go into the resist.<sup>16</sup> In this way,

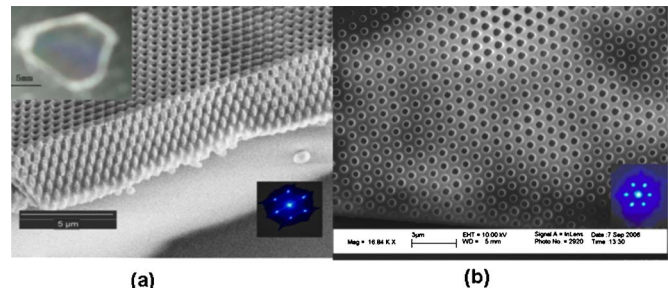


FIG. 3. (Color online) (a) Cleaved 3D photonic crystal on SU8 with a 1.1 s exposure with a light intensity of  $5.37\text{ mW}/\text{cm}^2$  at 325 nm. The upper-left corner inset shows the  $\text{cm}^2$  size photonic crystal. The lower-right corner inset shows the fcc-type (111) diffraction pattern. (b) SEM image of the (111) plane structure of AZ4620 with 10 s exposure with a light intensity of  $10.2\text{ mW}/\text{cm}^2$  at 442 nm. The lower-right corner inset shows the fcc-type (111) diffraction pattern.

we reversed the intensity distribution in the resist then the lower dosage of the surface part would compensate the longer etch time and maintain the surface structures.

In the experiments we used photoresist coated on a glass substrate for the 3D structure recording. The negative resist we used was SU8. After the spin coating, the substrate was baked at  $95^\circ\text{C}$  and we achieved a thickness of about  $10\ \mu\text{m}$ . The 325 nm line from the He–Cd CW laser was used to expose the sample. The index matching liquid was silicone oil which does not react with SU8. After the exposure we applied a postexposure bake at  $95^\circ\text{C}$ . The unexposed film was removed by propylene glycol methyl ether acetate and rinsed in DI water. For the positive photoresist, we used AZ4620. The coated film was about  $8\ \mu\text{m}$  thick. After the  $100^\circ\text{C}$  prebake, the 442 nm line from the He–Cd laser was used to expose the sample in the flipped fashion mentioned before. We used the same index matching liquid as in the SU8 case. No postexposure bake was necessary here.

Figures 3(a) and 3(b) show the scanning electron microscopy (SEM) images of the fabricated 3D polymer photonic crystal structures. The total area is just the size of the top surface of the prism. Figure 3(a) exhibits the whole size and a fracture of the cleaved 3D fcc-type structure using SU8. Figure 3(b) shows the structure on (111) plane of the AZ4620 resist. For the structures fabricated in the SU8 resist under the SEM observation, (111) in-plane and perpendicular lattice spacings are measured to be  $0.61$  and  $2.02\ \mu\text{m}$ , respectively. The simulation results showed the lattice spacings to be  $0.63$  and  $2.10\ \mu\text{m}$ , which are slightly larger than the fabrication results. Such differences can be attributed to the size error of the prism and the shrinkage of the photoresist after the bake process. As for the AZ4620 based structures, the lattice spacing in the (111) plane is  $0.82\ \mu\text{m}$  which is just 1.37 times the one we get in the SU8 case, and such a ratio is consistent with the ratio of the laser wavelengths we used for the two materials. From these observations we have shown that with careful modification to the conventional holographic fabrication process we can obtain a generic approach for fabricating submicron 3D photonic crystal using positive and negative photoresists. In addition, we used the 325 nm laser normally incident on the (111) plane of 3D photonic crystals in both materials to observe the diffraction patterns which are equivalent to x-ray diffraction normal to the (111) plane of a fcc single crystal.<sup>17</sup> The diffractions from both materials exhibit similar patterns as shown of the insets of both figures in Fig. 3 except for different first order diffrac-

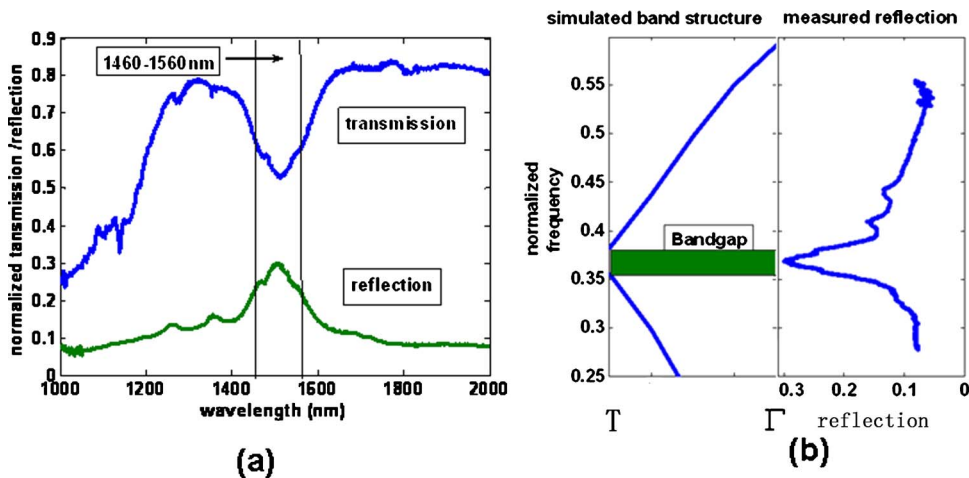


FIG. 4. (Color online) (a) Normalized Fourier transform infrared transmission and reflection spectra in the  $[111]$  direction. (b) Comparison of the calculated band and the measured reflection spectrum shows good agreement for the  $S+C$  band (1460–1565 nm). The right-hand side has the same reflection spectrum as in (a).

tion angles of  $35^\circ$  and  $23^\circ$  due to the different periodicities. The periods calculated from the diffraction angles are in good agreement with the SEM measurements and such diffraction patterns further assure us of the formation of good 3D periodic microstructures.

We have characterized the optical transmission and reflection properties of the SU8 photonic crystals with an estimated filling factor of 45% using a Fourier transform infrared spectrometer. The surface of the sample, which was the (111) plane, was aligned perpendicular to the optical axis in the setup. In Fig. 4(a) the dip in the transmission and the peak in the reflection spectrum both occur around  $1.5 \mu\text{m}$  and the band covers 1460–1565 nm. In addition, the bulk SU8 transmission is almost 100% in the whole spectrum range and it is an indication that the fine structures in the spectrum are not related to the absorption of the SU8 material. Compared with the band structure in the  $[111]$  propagation direction calculated by plane wave expansion, the position of the dip in the transmission is in good agreement with the simulation. Due to the roughness of the structures on a 10 nm scale we have also observed a decrease of the transmission towards shorter wavelength.

In conclusion we have demonstrated the fabrication of submicron 3D polymer photonic crystal structure for both negative and positive photoresists. Using this method and with similar lattice constant one can fabricate photonic crystals to demonstrate other effects such as superprism and supercollimator. And by backfilling the porous 3D structure with liquid crystal or electro-optic polymer, tunable photonic crystal devices can be generated.

This work is supported by the Air Force Research Laboratory. The authors thank R. L. Nelson and J. W. Haus for helpful discussions.

<sup>1</sup>S. John, *Phys. Rev. Lett.* **58**, 2486 (1987).

<sup>2</sup>J. D. Joannopoulos, R. D. Meade, and J. N. Winn, *Photonic Crystals* (Princeton University Press, Princeton, NJ, 1995).

<sup>3</sup>W. Jiang and R. T. Chen, *Phys. Rev. Lett.* **91**, 213901 (2003).

<sup>4</sup>W. Jiang, R. T. Chen, and X. Lu, *Phys. Rev. B* **71**, 245115 (2005).

<sup>5</sup>Y. Jiang, W. Jiang, L. Gu, X. Chen, and R. T. Chen, *Appl. Phys. Lett.* **87**, 221105 (2005).

<sup>6</sup>H. Benisty, J. Lourtioz, A. Chelnokov, S. Combrié, and X. Checoury, *Proc. IEEE* **94**, 997 (2006).

<sup>7</sup>L. J. Guo, *J. Phys. D* **37**, 123 (2004).

<sup>8</sup>K. Aoki, H. T. Miyazaki, H. Hirayama, K. Inoshita, and T. Baba, *Nat. Mater.* **2**, 117 (2003).

<sup>9</sup>M. Deubel, G. V. Freymann, M. Wegner, S. Pereira, K. Busch, and C. M. Soukoulis, *Nat. Mater.* **3**, 444 (2004).

<sup>10</sup>M. Campbell, D. N. Sharp, M. T. Harrison, R. G. Denning, and A. J. Turberfield, *Nature (London)* **404**, 53 (2000).

<sup>11</sup>L. Z. Cai, X. L. Yang, and Y. R. Wang, *Opt. Lett.* **27**, 900 (2002).

<sup>12</sup>I. Divliansky, T. S. Mayer, K. S. Holliday, and V. H. Crespi, *Appl. Phys. Lett.* **82**, 1667 (2003).

<sup>13</sup>L. Wu, Y. Zhong, C. T. Chan, K. S. Wong, and G. P. Wang, *Appl. Phys. Lett.* **86**, 241102 (2005).

<sup>14</sup>R. C. Rumpf and E. G. Johnson, *J. Opt. Soc. Am. A* **21**, 1803 (2004).

<sup>15</sup>T. Kondo, S. Juodkazis, and H. Misawa, *Appl. Phys. A: Mater. Sci. Process.* **81**, 1583 (2005).

<sup>16</sup>R. T. Chen, L. Sadovnik, T. M. Aye, and T. Jansson, *Opt. Lett.* **15**, 869 (1990).

<sup>17</sup>N. W. Aschcroft and N. D. Mermin, *Solid State Physics* (Saunders College, Philadelphia, 1976).